The Early Stages of the Phase Separation Dynamics in Polydisperse Polymer Blends

C. Huang*,† and M. Olvera de la Cruz†,‡

Departments of Materials Science and Engineering and Chemical Engineering, Northwestern University, Evanston, Illinois 60208

Received February 15, 1994; Revised Manuscript Received April 28, 1994•

ABSTRACT: The thermodynamics and the dynamics of incompatible polydisperse polymer blends are analyzed. The free energy is constructed following the Flory–Huggins approach, where the degree of incompatibility is characterized by the Flory interaction parameter χ. The Cahn–Hilliard approximation is used to analyze the early stages of spinodal decomposition dynamics of a polymer blend quenched into the unstable region. A blend of polydisperse A polymers with the Schulz–Flory distribution and monodisperse B polymers is analyzed by treating polymer A as a one-, two-, and three-component system with a weight-average degree of polymerization and a polydispersity index, which we refer to as two-, three-, and four-component models, respectively. The thermodynamics and the dynamics of incompatible monodisperse A–monodisperse B polymer blends are consistent no matter which model is used. When polymer A is polydisperse, however, $[S(k,t)-S(k,0)]/S(k,0)$, where $S(k,t)$ is the characteristic structure function, is definitely different in the three different models due to kinetic effects. The differences are dependent on the functional form of the Onsager coefficients. For wavevector-independent Onsager coefficients, the reduced wavevector for which $[S(k,t)-S(k,0)]/S(k,0)$ is a maximum, k^*_{peak}, is always equal to $1/\sqrt{2}$ in the two-component model, while k^*_{peak} increases as χ increases in the three- and four-component models. While for wavevector-dependent Onsager coefficients, k^*_{peak} decreases as χ increases in the three different component models. As $\chi \to \infty$, the difference in k^*_{peak} between two- and three-component models and between three- and four-component models is 0.05 and 0.02, respectively, independent of the weight-average degree of polymerization when the polydispersity index of polymer A is equal to 2.0. When the polydispersity index of polymer A is reduced to 1.5, the difference in k^*_{peak} becomes 0.04 and 0.01, respectively.

I. Introduction

Since most commercial polymers are polydisperse, a description of the thermodynamics and the dynamics of the phase separation process that includes polydispersity effects is required. Incompatible A–B polymer blends have long been described by the mean field theory which assumes that the chains obey Gaussian statistics and the monomers are placed at random in space without correlations. Edwards[1] showed that long polymer chains in the molten state obey Gaussian statistics. Furthermore, de Gennes pointed out[2] that the mean field theory is a good approach for incompatible high degree of polymerization (P) polymer blends. When a polydisperse polymer blend is analyzed, the mean field theory may not be applicable since the short chains may swell the long chains. However the swelling effect can be neglected if the polydisperse polymer samples of high weight-average degree of polymerization are chosen to have a small fraction of short chains. To study the effect of polydispersity on the thermodynamics and the dynamics of the phase separation process of incompatible polymer blends, we concentrate our attention on a blend of an incompatible polydisperse polymer A sample with weight-average degree of polymerization P_{Aw} and with polydispersity index γ_A and a monodisperse polymer B sample with degree of polymerization P_B. We construct the thermodynamics using the Flory–Huggins mean field theory. The free energy of mixing per lattice site is therefore given by

$$\Delta f = K_B T\left[\sum_P \frac{\varphi^\circ_A P \ln \varphi^\circ_{AP}}{P} + \frac{\varphi^\circ_B \ln \varphi^\circ_B}{P_B} + \chi \varphi^\circ_A \varphi^\circ_B\right] \quad (1)$$

† Department of Materials Science and Engineering.
‡ Department of Chemical Engineering.
• Abstract published in *Advance ACS Abstracts*, June 1, 1994.

where

$$\chi = \frac{Z}{K_B T}\left(\omega_{AB} - \frac{1}{2}(\omega_{AA} + \omega_{BB})\right)$$

is the usual Flory interaction parameter and φ°_A and φ°_B are the average compositions of polymers A and B, respectively. In eq 1, φ°_{AP} is the average composition of polymer A whose degree of polymerization is equal to P. In the χ–φ plane, there exists a spinodal curve which is the boundary between the metastability and instability of the system. Inside the spinodal curve, the mixture is always unstable and breaks up into two phases by spinodal decomposition.[3,4]

We use the n-component system method developed by de Fontaine[5] to find the instability limits and the critical point. In an A–B blend where the polymer A sample has $n-1$ different degrees of polymerization and polymer B is monodisperse, an $(n-1)^*(n-1)$ matrix with matrix elements f_{ij} defined as

$$f_{ij} = \left(\frac{\partial}{\partial \varphi_i} - \frac{\partial}{\partial \varphi_n}\right)\left(\frac{\partial}{\partial \varphi_j} - \frac{\partial}{\partial \varphi_n}\right)(\Delta f) \quad (2)$$

must be obtained to find the instability limits of the blend. The effect of polydispersity on the critical point, on the other hand, is easily obtained.[6] The critical point is given by

$$\varphi^\circ_{Ac} = \left(1 + \frac{P_{Aw}}{P_B^{1/2} P_{Az}^{1/2}}\right)^{-1}$$
$$2\chi_c = \left(\frac{1}{P_{Az}^{1/2}} + \frac{1}{P_B^{1/2}}\right)\left(\frac{P_{Az}^{1/2}}{P_{Aw}} + \frac{1}{P_B^{1/2}}\right) \quad (3)$$

where P_{Az} is the z-average degree of polymerization of

0024-9297/94/2227-4231$04.50/0

polymer A defined by

$$P_{Az} = \frac{\sum_P W(P) \times P^2}{\sum_P W(P) \times P} \tag{4}$$

$W(P)$ is the weight distribution of polymer A. This result will be corroborated with a technique described later.

Our dynamics studies are concentrated on the early stages of the phase separation process by spinodal decomposition. The theory of spinodal decomposition dynamics for binary systems has been developed by Cahn and Hilliard.[3,4] The kinetics of spinodal decomposition are described by a nonlinear differential equation for the rate of change of the composition. For simplicity, Cahn and Hilliard developed a linearized differential equation to describe the early stages of the phase separation, which was proved to be correct later by Langer, Baron, and Miller[7] in systems well described by the mean field theory. Cook[8] included in the linearized Cahn–Hilliard theory the effect of the thermal fluctuations, or the "heat bath" term. This term, however, can be neglected if the system is quenched into the deep region for which χ is much larger than χ_c. The most useful point of the linearized Cahn–Hilliard theory is that a time-dependent structure function, proportional to the scattering intensity by small angle X-ray scattering experiments,[9] can be derived from it.

de Fontaine has developed the linearized Cahn–Hilliard equations for a multicomponent system. These equations could be used to analyze the early stages of the spinodal decomposition process of the incompatible polydisperse A–monodisperse B polymer blends with n components. In practice, however, his approach generates $n(n-1)/2$ independent partial structure functions and the numerical values of these partial structure functions are difficult to get since a $n(n-1)/2 \times n(n-1)/2$ matrix must be constructed. Therefore, we try here to approach the real system by treating the polydisperse polymer A as a mixture of one, two, and three monodisperse polymer samples and constructing in this way the spinodal decomposition dynamics as two-, three-, and four-component models, respectively. It should be noted that the idea of the three-component model was first proposed by Takenaka and Hashimoto[10] to see the effect of polydispersity on the validity of the dynamic scaling law in the late stage of spinodal decomposition. However they use the Onsager coefficients derived by assuming that in the incompressible liquid the motion of the monomers occurs only by exchanging their positions. Here, instead, we use vacancy driven diffusion (see section II).

In section II we find the compositions that describe the mean field thermodynamics and Cahn–Hilliard dynamics of polydisperse polymer A–monodisperse polymer B blends. We construct the two-, three-, and four-component models in section II.1–3, respectively. In section II.1, polydisperse polymer A is regarded as a monodisperse polymer with degree of polymerization equal to P_{Aw}. The early stages of spinodal decomposition dynamics for different χ values will be obtained using the Cahn–Hilliard approximation for binary systems. In section II.2, the polydisperse polymer A is assumed to be composed of two monodisperse polymer samples, 1 and 2. The method to obtain the compositions of samples 1 and 2 will be described in this section. Then we analyze the thermodynamics and the dynamics of the systems described in section II according to the Cahn–Hilliard approximation for ternary systems and compare with the results in the two-component model. In section II.3, polymer A was considered to be composed of three monodisperse polymer samples, 1–3. We describe the method to obtain the compositions of these samples in this section. The thermodynamics and the dynamics will be analyzed in the four-component model and will be compared with the two- and three-component models. In section II, we also describe the thermodynamics and the dynamics of incompatible monodisperse A–B polymer blends in the different models for a comparison with polydisperse A–monodisperse B polymer blends. The discussion and conclusions are given in sections III and IV, respectively.

II. Theory and Results

Incompatible polydisperse polymer A–monodisperse polymer B blends are described by the weight-average degree of polymerization and polydispersity index of polymer A (P_{Aw} and γ_A, respectively), and degree of polymerization of polymer B (P_B). The weight distribution $W(P)$ of polymer A is described by the Schulz–Flory distribution:[11,12]

$$W(P) = \frac{\eta^{\sigma+1}P^{\sigma}}{\Gamma(\sigma+1)}e^{-\eta P} \qquad P = 1, 2, ..., \infty \tag{5}$$

where η and σ are constants related to P_{Aw} and γ_A. If σ is an integer,

$$P_{Aw} = \frac{\sigma+1}{\eta} \tag{6}$$

$$\gamma_A = \frac{P_{Aw}}{P_{An}} = 1 + \frac{1}{\sigma} \tag{7}$$

The weight distribution of polymer A of a given P_{Aw} and γ_A can be determined using eqs 6 and 7 by solving for σ and η. The critical compositions are determined by using eqs 3 and 4. Two incompatible polymer blend systems (1 and 2) are analyzed. System 1 has

$$P_{Aw} = P_B = 1000$$

$$\gamma_A = 2.0$$

$$\varphi^{\circ}_{Ac} = 0.5505 \tag{8}$$

$$\varphi^{\circ}_{Bc} = 0.4495$$

$$\chi_c P = 2.020\,62$$

and system 2

$$P_{Aw} = P_B = 1000$$

$$\gamma_A = 1.5$$

$$\varphi^{\circ}_{Ac} = 0.5359 \tag{9}$$

$$\varphi^{\circ}_{Bc} = 0.4641$$

$$\chi_c P = 2.010\,36$$

The monodisperse A–B polymer blend ($\gamma_A = 1$) to be analyzed for comparison with the incompatible polydis-

perse A–monodisperse B polymer blends has

$$P_A = P_B = 1000$$
$$\varphi^\circ_{Ac} = 0.5$$
$$\varphi^\circ_{Bc} = 0.5 \quad (10)$$
$$\chi_c P = 2$$

II.1. Two-Component Model. In this model the polydisperse polymer A is characterized by the degree of polymerization P_{Aw}. We can construct then the diffusion equations as in a binary system. Two theories have been used to construct the linearized Cahn–Hilliard differential equations in monodisperse polymer blends, one proposed by de Gennes[13] and the other by Kramer.[14] We adopt the results of Kramer et al. who propose that there is a net vacancy flux during the diffusion processes with the constraint of local thermal equilibrium of vacancies, which has been shown[15] to agree better with experiments.[16] Therefore, the diffusion fluxes of polymers A and B are

$$J_A = -[(1-\varphi^\circ_A)M_A\nabla\mu_A - \varphi^\circ_A M_B\nabla\mu_B] \quad (11.a)$$

$$J_B = -[-\varphi^\circ_B M_A\nabla\mu_A + (1-\varphi^\circ_B)M_B\nabla\mu_B] \quad (11.b)$$

where M_A and M_B are Onsager coefficients for the A and B monomers. Since $J_A + J_B \equiv 0$, there is only one independent diffusion flux. Let us choose J_A. Using the conservation law, we get

$$\frac{\partial}{\partial t}[\varphi_A(r,t)] = \nabla[(1-\varphi^\circ_A)M_A\nabla\mu_A - \varphi^\circ_A M_B\nabla\mu_B] \quad (12)$$

where M_A and M_B can be expressed in terms of the diffusion coefficient D_o of each monomer as

$$M_i = \frac{\varphi^\circ_i}{P_i} \times \frac{(1-\exp(-k^2R_{gi}^2))}{k^2R_{gi}^2}\frac{D_oP_e}{K_BT} \quad i = A, B \quad (13.a)$$

where P_e is the effective number of monomers per entanglement length and R_{gi} is the radius of gyration. In eq 13.a we used the results of Pincus[17,18] for the wavevector dependence of the Onsager coefficients M_i in the reptation model. Though in the work of Pincus the mobility was assumed to obey de Gennes' model, it can be used in Kramer's model. When $kR_{gi} \ll 1$, the Onsager coefficients become k-independent and reduce to

$$M_i = \frac{\varphi^\circ_i}{P_i} \times \frac{D_oP_e}{K_BT} \quad (13.b)$$

By using the Gibbs–Duhem equation and substituting for the chemical potentials, we can rewrite eq 12 in the form

$$\frac{\partial}{\partial t}[\varphi_A(r,t)] = M[f''\nabla^2(\varphi_A(r,t)) - 2\kappa\nabla^4(\varphi_A(r,t))] \quad (14)$$

where

$$M = [(1-\varphi^\circ_A)^2M_A + \varphi^{\circ 2}_A M_B] \quad (15)$$

f'' is defined as the second derivative of the free energy, and κ is the gradient-energy coefficient.

Rundman and Hilliard[9] have shown that small angle X-ray scattering is a good technique to test the theory of spinodal decomposition. The scattering intensity is directly proportional to the structure function $S(k,t)$ which is the Fourier transformation of the pair correlation function $C(r,t)$. The structure functions are defined as

$$S_{ij}(k,t) = \frac{1}{a^3}\langle\varphi_i(k,t)\varphi^*_j(k,t)\rangle = \frac{1}{V}\int_V C_{ij}(r,t)e^{ik\cdot r}\,d^3r \quad (16.a)$$

where

$$C_{ij}(r-r',t) = \langle\varphi_i(r,t)\varphi_j(r',t)\rangle \quad (16.b)$$

$$\varphi_i(k,t) = \frac{1}{V}\int_V\varphi_i(r,t)e^{ik\cdot r}\,d^3r \quad (16.c)$$

and $\langle ... \rangle$ denotes the thermal average. Under conditions of incompressibility, there is only one independent structure function.

$$S(k,t) = S_{AA}(k,t) = S_{BB}(k,t) = -S_{AB}(k,t)$$

The time dependence equation for the scattering function can be obtained by multiplying eq 14 by $\varphi_A(r',t)$ to get the relationship between $C_{ij}(r,t)$ and the derivative of $C_{ij}(r,t)$ with respect to time and taking the Fourier transform,

$$\frac{\partial}{\partial t}S(k,t) = -2Mk^2(f'' + 2\kappa k^2)S(k,t) \quad (17)$$

which is known as the Cahn–Hilliard equation. In the Cahn–Hilliard–Cook approximation a "heat bath" term $Q(k,t) = 2Mk^2K_BT$ must be added to the right hand side of eq 17. The heat bath term is very important for quenches in the one-phase region or for shallow quenches, very near the χ_c. As the final χ, χ_f, increases to a value far from χ_c, the effect of the heat bath is negligible. Since we will only concentrate on deep quenches, into a region of $\chi_f \gg \chi_c$, we neglect the heat bath term. Therefore, the solution of $S(k,t)$ becomes

$$S(k,t) = e^{-2Mk^2(f''+2\kappa k^2)t}S(k,0) \quad (18)$$

where $S(k,0)$ represents the initial structure function, which is related to the initial χ, χ_o, in the one-phase region where $\chi_o \ll \chi_c$. In polydisperse polymer blends (see Appendix),

$$f'' = K_BT\left(\frac{1}{\varphi^\circ_A P_{Aw}} + \frac{1}{\varphi^\circ_B P_B} - 2\chi\right) \quad (19)$$

and

$$\kappa = K_BT \times \frac{a^2}{36}\left(\frac{\overline{P_A^2}}{\varphi^\circ_A P_{Aw}} + \frac{1}{\varphi^\circ_B}\right) \quad (20)$$

In Figures 1–3 and Figures 4–6 we plot $\Delta S / S(k,0)$ versus k^* for the polydisperse A–monodisperse B systems 1 and 2 (see eqs 8 and 9), respectively, in the two-component model, where $\Delta S = S(k,t) - S(k,0)$ and k^* is defined as the ratio of k to k_c where k_c is given by $f'' + 2\kappa k_c^2 = 0$. In Figure 7 we show $\Delta S/S(k,0)$ versus k^* for the monodisperse A–B system (see eq 10) quenched to different χ_f values. As observed, k^*_{peak} decreases as χ_f increases.

II.2. Three-Component Model. In this model, the polydisperse A polymer is considered to be composed of two polydisperse polymer samples, 1 and 2, having weight-average degree of polymerizations equal to P_{1w} and P_{2w}, respectively. The average compositions φ°_1 and φ°_2 are constructed to be the same. Polymer sample 1 is composed of the chains whose degrees of polymerization are less than P_o, and polymer sample 2 is composed of the chains longer

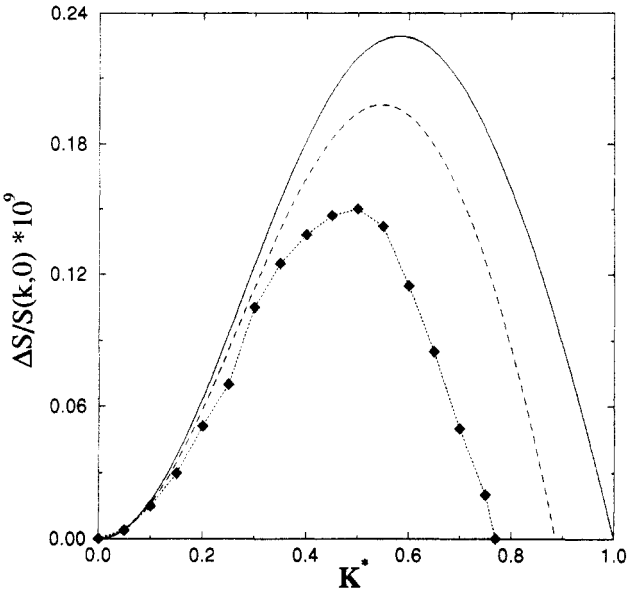

Figure 1. Normalized structure function of the polydisperse polymer blend 1 described in eq 8 for quenches from $\chi_o = 0$ to $\chi_f P = 5.0$ for $t = 1$. The symbols —, - - -, and ♦···♦ correspond to the two-, three-, and four-component models, respectively, and $k^*_{peak} = 0.58$, 0.55, and 0.53, respectively.

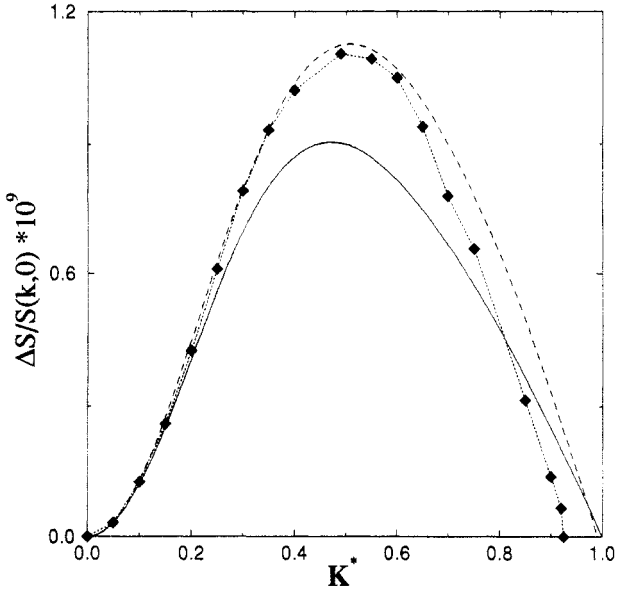

Figure 2. Normalized structure function of the polydisperse polymer blend 1 described in eq 8 for quenches from $\chi_o = 0$ to $\chi_f P = 10$ for $t = 1$. The symbols —, - - -, and ♦···♦ correspond to the two-, three-, and four-component models, respectively, and $k^*_{peak} = 0.47$, 0.51, and 0.49, respectively.

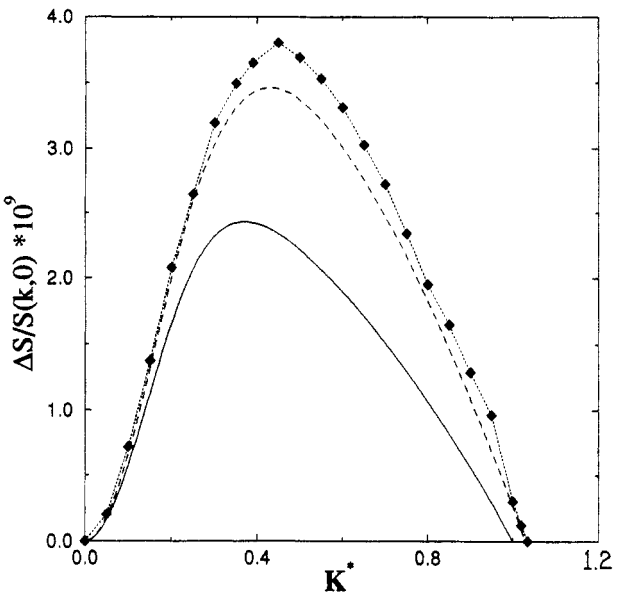

Figure 3. Normalized structure function of the polydisperse polymer blend 1 described in eq 8 for quenches from $\chi_o = 0$ to $\chi_f P = 20$ for $t = 1$. The symbols —, - - -, and ♦···♦ correspond to the two-, three-, and four-component models, respectively, and $k^*_{peak} = 0.37$, 0.43, and 0.45, respectively.

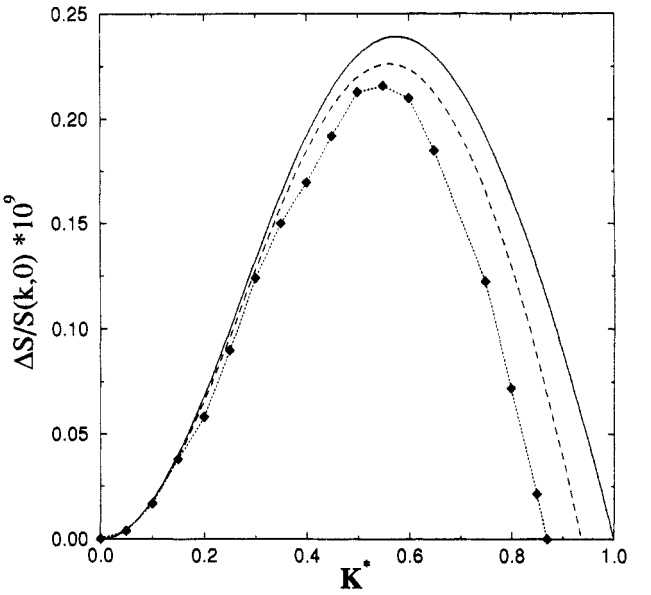

Figure 4. Normalized structure function of the polydisperse polymer blend 2 described in eq 9 for quenches from $\chi_o = 0$ to $\chi_f P = 5.0$ for $t = 1$. The symbols —, - - -, and ♦···♦ correspond to the two-, three-, and four-component models, respectively, and $k^*_{peak} = 0.57$, 0.56, and 0.55, respectively.

than P_o, where P_o is given by

$$\sum_{P=1}^{P=P_o} W_A(P) = \sum_{P=P_o}^{P=\infty} W_A(P) = \frac{1}{2} \tag{21}$$

Therefore, P_{1w} and P_{2w} are given by

$$P_{1w} = \frac{\sum_{P=1}^{P=P_o} W_A(P) \times P}{\sum_{P=1}^{P=P_o} W_A(P)} \tag{22.a}$$

$$P_{2w} = \frac{\sum_{P=P_o}^{P=\infty} W_A(P) \times P}{\sum_{P=P_o}^{P=\infty} W_A(P)} \tag{22.b}$$

where $W_A(P)$ is a normalized weight distribution.

The free energy of mixing per lattice site is

$$\Delta f = K_B T\left[\frac{\varphi_1^\circ \ln \varphi_1^\circ}{P_{1w}} + \frac{\varphi_2^\circ \ln \varphi_2^\circ}{P_{2w}} + \frac{\varphi_3^\circ \ln \varphi_3^\circ}{P_3} + \chi\varphi_1^\circ\varphi_3^\circ + \chi\varphi_2^\circ\varphi_3^\circ\right] \tag{23}$$

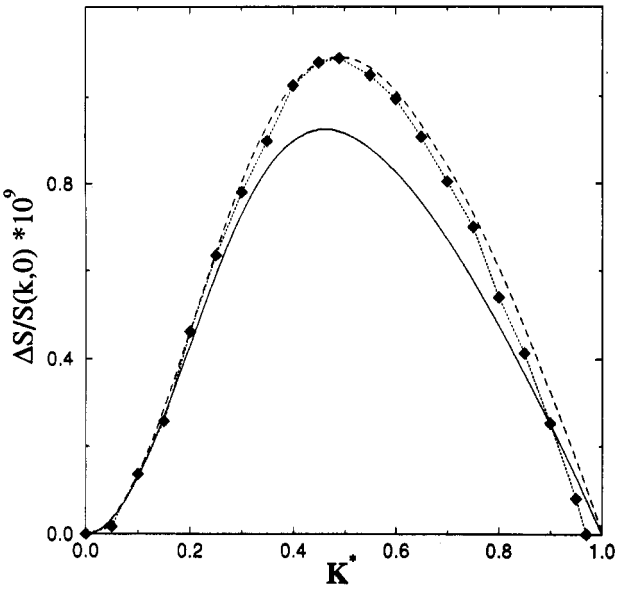

Figure 5. Normalized structure function of the polydisperse polymer blend 2 described in eq 9 for quenches from $\chi_o = 0$ to $\chi_t P = 10$ for $t = 1$. The symbols —, - - -, and ♦···♦ correspond to the two-, three-, and four-component models, respectively, and $k^*_{peak} = 0.46$, 0.49, and 0.49, respectively.

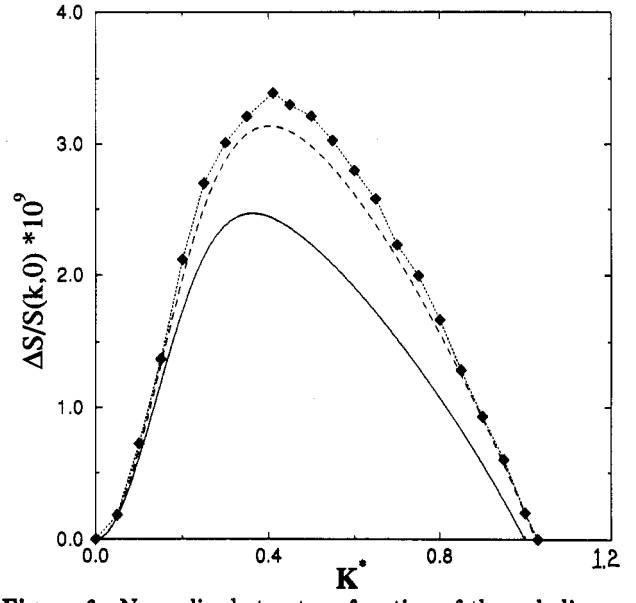

Figure 6. Normalized structure function of the polydisperse polymer blend 2 described in eq 9 for quenches from $\chi_o = 0$ to $\chi_t P = 20$ for $t = 1$. The symbols —, - - -, and ♦···♦ correspond to the two-, three-, and four-component models, respectively, and $k^*_{peak} = 0.36$, 0.40, and 0.41, respectively.

The spinodal surface is given by

$$\begin{vmatrix} f_{11} & f_{12} \\ f_{21} & f_{22} \end{vmatrix} = 0$$

with

$$f_{11} = K_B T\left[\frac{1}{\phi_1^\circ P_{1w}} + \frac{1}{\phi_3^\circ P_3} - 2\chi\right] \quad (24.a)$$

$$f_{12} = f_{21} = K_B T\left[\frac{1}{\phi_3^\circ P_3} - 2\chi\right] \quad (24.b)$$

$$f_{22} = K_B T\left[\frac{1}{\phi_2^\circ P_{2w}} + \frac{1}{\phi_3^\circ P_3} - 2\chi\right] \quad (24.c)$$

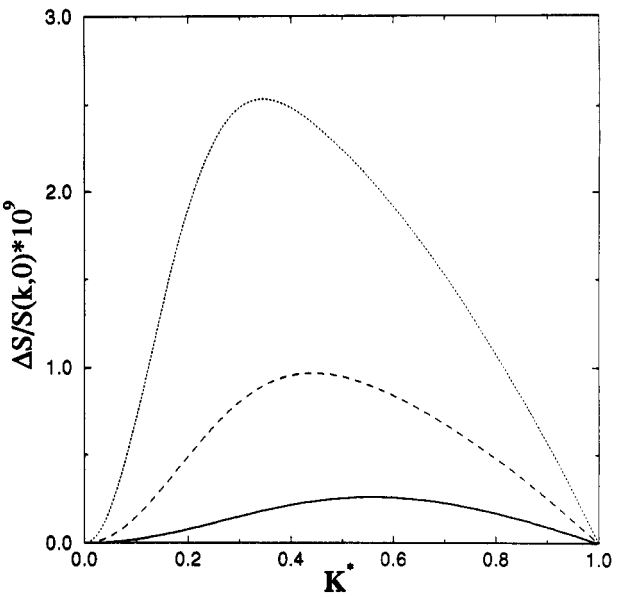

Figure 7. Normalized structure function of the monodisperse polymer blend described in eq 10 for quenches from $\chi_o = 0$ to $\chi_t P$ for $t = 1$. The symbols —, - - -, and ··· correspond to $\chi_t P = 5.0$, 10, and 20, respectively, and $k^*_{peak} = 0.56$, 0.44, and 0.34, respectively.

Since $\phi_1^\circ = \phi_2^\circ = \phi_A^\circ/2$ and $\phi_1^\circ P_{1w} + \phi_2^\circ P_{2w} = \phi_A^\circ P_{Aw}$,

$$2\chi_S = \frac{1}{\phi_1^\circ P_{1w} + \phi_2^\circ P_{2w}} + \frac{1}{\phi_3^\circ P_3} = \frac{1}{\phi_A^\circ P_{Aw}} + \frac{1}{\phi_B^\circ P_B} \quad (25)$$

which is consistent with the result for the two-component model. Therefore, the critical compositions and critical χ in the three-component model of the polydisperse A and monodisperse B polymer blend can be obtained from

$$\phi_{1c}^\circ = \phi_{2c}^\circ = \frac{\phi_{Ac}^\circ}{2}$$

$$\phi_{3c}^\circ = \phi_{Bc}^\circ \quad (26)$$

$$\chi_c^{3\text{-comp}} = \chi_c^{2\text{-comp}}$$

Therefore, system 1 analyzed in the three-component model will be

$$P_{1w} = 474$$

$$P_{2w} = 1526$$

$$P_3 = 1000 \quad (27)$$

$$\phi_{1c}^\circ = \phi_{2c}^\circ = 0.275\,25$$

$$\phi_{3c}^\circ = 0.4495$$

$$\chi_c P = 2.020\,62$$

System 2 will be

$$P_{1w} = 560$$

$$P_{2w} = 1440$$

$$P_3 = 1000 \quad (28)$$

$$\phi_{1c}^\circ = \phi_{2c}^\circ = 0.267\,95$$

$$\varphi_{3c}^{\circ} = 0.4641$$

$$\chi_c P = 2.010\,36$$

With this construction, when polymer A is monodisperse, $P_{1w} = P_{2w} = P_A$, the monodisperse system described in eq 10 would be

$$P_{1w} = 1000$$

$$P_{2w} = 1000$$

$$P_3 = 1000 \tag{29}$$

$$\varphi_{1c}^{\circ} = \varphi_{2c}^{\circ} = 0.25$$

$$\varphi_{3c}^{\circ} = 0.5$$

$$\chi_c P = 2$$

In the three-component model, the diffusion equations can be derived as follows:

$$J_1 = -[(1-\varphi_1^{\circ})M_1\nabla\mu_1 - \varphi_1^{\circ}M_2\nabla\mu_2 - \varphi_1^{\circ}M_3\nabla\mu_3] \tag{30.a}$$

$$J_2 = -[-\varphi_2^{\circ}M_1\nabla\mu_1 + (1-\varphi_2^{\circ})M_2\nabla\mu_2 - \varphi_2^{\circ}M_3\nabla\mu_3] \tag{30.b}$$

$$J_3 = -[-\varphi_3^{\circ}M_1\nabla\mu_1 - \varphi_3^{\circ}M_2\nabla\mu_2 + (1-\varphi_3^{\circ})M_3\nabla\mu_3] \tag{30.c}$$

There are two independent fluxes since $J_1 + J_2 + J_3 \equiv 0$. Let us say J_1 and J_2. By using the Gibbs–Duhem equation and the conservation law of the diffusion, we get

$$\frac{\partial}{\partial t}[\varphi_1(r,t)] = M_{11}\nabla^2(\mu_1-\mu_3) + M_{12}\nabla^2(\mu_2-\mu_3) \tag{31.a}$$

$$\frac{\partial}{\partial t}[\varphi_2(r,t)] = M_{21}\nabla^2(\mu_1-\mu_3) + M_{22}\nabla^2(\mu_2-\mu_3) \tag{31.b}$$

where

$$M_{11} = (1-\varphi_1^{\circ})^2M_1 + \varphi_1^{\circ 2}M_2 + \varphi_1^{\circ 2}M_3 \tag{32.a}$$

$$M_{12} = M_{21} = -(1-\varphi_1^{\circ})\varphi_2^{\circ}M_1 - (1-\varphi_2^{\circ})\varphi_1^{\circ}M_2 + \varphi_1^{\circ}\varphi_2^{\circ}M_3 \tag{32.b}$$

$$M_{22} = \varphi_2^{\circ 2}M_1 + (1-\varphi_2^{\circ})^2M_2 + \varphi_2^{\circ 2}M_3 \tag{32.c}$$

In eq 31, $\mu_i - \mu_3$ can be expressed in terms of f_{ij} and the gradient-energy coefficients κ_{ij}.[3]

In an n-component system f_{ij} and κ_{ij} are derived as follows: The total free energy of the n-component system F is

$$F = \int_V \left[f(\varphi_i;i=1,2,...,n) + \frac{1}{2}\sum_{i,j=1}^{n}\left(\nabla\varphi_i\nabla\varphi_j\frac{\partial^2}{\partial\nabla\varphi_i\partial\nabla\varphi_j}\right)f(\varphi_i;i=1,...,n)\right] dV \tag{33}$$

and the chemical potential μ_i is given by

$$\mu_i = \frac{\partial}{\partial\varphi_i}f(\partial_i;i=1,2,...,n) - \sum_{j=1}^{n}\left[\nabla^2\varphi_j \times \frac{\partial^2}{\partial\nabla\varphi_i\partial\nabla\varphi_j}\right]f(\varphi_i;i=1,2,...,n) \tag{34}$$

A Taylor expansion of $(\partial/\partial\varphi_i)f(\varphi_i;i=1,2,...,n)$ about $\varphi_i = \varphi_i^{\circ}$ gives

$$\frac{\partial}{\partial\varphi_i}f(\varphi_i;i=1,2,...,n) = \frac{\partial f_o}{\partial\varphi_i} + \sum_{j=1}^{n}\frac{\partial^2 f_o}{\partial\varphi_i\partial\varphi_j}(\varphi_j - \varphi_j^{\circ}) \tag{35}$$

where $f_o = f(\varphi_i^{\circ};i=1,2,...,n)$ and φ_i° denotes the average composition of the ith component. Since $\varphi_1(r,t) + \varphi_2(r,t) + ... + \varphi_n(r,t) \equiv 1$, $\varphi_n - \varphi_n^{\circ}$ and $\nabla^2\varphi_n$ can be expressed in terms of the other $n-1$ components. Therefore, the chemical potential becomes

$$\mu_i = \frac{\partial f_o}{\partial\varphi_i} + \sum_{j=1}^{n-1}\left(\frac{\partial^2 f_o}{\partial\varphi_i\partial\varphi_j} - \frac{\partial^2 f_o}{\partial\varphi_i\partial\varphi_n}\right)(\varphi_j - \varphi_j^{\circ}) - 2\sum_{j=1}^{n-1}(\bar{\kappa}_{ij} - \bar{\kappa}_{in})\nabla^2\varphi_j \tag{36}$$

where

$$\bar{\kappa}_{ij} = \frac{1}{2}\frac{\partial^2 f(\varphi_i;i=1,2,...,n)}{\partial\nabla\varphi_i\partial\nabla\varphi_j} \tag{37}$$

and

$$\mu_i - \mu_n = \frac{\partial f_o}{\partial\varphi_i} - \frac{\partial f_o}{\partial\varphi_n} + \sum_{j=1}^{n-1}f_{ij}(\varphi_j - \varphi_j^{\circ}) - 2\sum_{j=1}^{n-1}\kappa_{ij}\nabla^2\varphi_j \tag{38}$$

where f_{ij} is given in eq 2 and

$$\kappa_{ij} = \bar{\kappa}_{ij} - \bar{\kappa}_{in} - \bar{\kappa}_{nj} + \bar{\kappa}_{nm} \tag{39}$$

In polymer blends for the three-component model, f_{ij} and κ_{ij} can be obtained using the same steps as the two-component model (see Appendix), f_{ij} are given in eq 24, and

$$\kappa_{11} = K_B T\left[\frac{a^2}{36}\times\left(\frac{\overline{P_1^2}}{\varphi_1^{\circ}P_{1w}^2} + \frac{1}{\varphi_3^{\circ}}\right)\right] \tag{40.a}$$

$$\kappa_{12} = \kappa_{21} = K_B T\left[\frac{a^2}{36}\times\left(\frac{1}{\varphi_3^{\circ}}\right)\right] \tag{40.b}$$

$$\kappa_{22} = K_B T\left[\frac{a^2}{36}\times\left(\frac{\overline{P_2^2}}{\varphi_2^{\circ}P_{2w}^2} + \frac{1}{\varphi_3^{\circ}}\right)\right] \tag{40.c}$$

Thus, the time dependence composition equations become

$$\frac{\partial}{\partial t}\varphi_1(r,t) = (M_{11}f_{11} + M_{12}f_{21})\nabla^2\varphi_1(r,t) - 2(M_{11}\kappa_{11} + M_{12}\kappa_{21})\nabla^4\varphi_1(r,t) + (M_{11}f_{12} + M_{12}f_{22})\nabla^2\varphi_2(r,t) - 2(M_{11}\kappa_{12} + M_{12}\kappa_{22})\nabla^4\varphi_2(r,t) \tag{41.a}$$

$$\frac{\partial}{\partial t}\varphi_2(r,t) = (M_{21}f_{11} + M_{22}f_{21})\nabla^2\varphi_1(r,t) - 2(M_{21}\kappa_{11} + M_{22}\kappa_{21})\nabla^4\varphi_1(r,t) + (M_{21}f_{12} + M_{22}f_{22})\nabla^2\varphi_2(r,t) - 2(M_{21}\kappa_{12} + M_{22}\kappa_{22})\nabla^4\varphi_2(r,t) \tag{41.b}$$

Since there are two independent compositions $\varphi_1(r,t)$ and $\varphi_2(r,t)$, there are three partial structure functions $S_{11}(k,t)$, $S_{12}(k,t)$, and $S_{22}(k,t)$. The differential equations for the three partial structure functions in a ternary system were proposed by Hoyt.[19] First we multiply eq 41 by $\varphi_1(r',t)$ and $\varphi_2(r',t)$ to get the equations of the time derivatives of the pair correlation functions. The Fourier transforms of

these equations are

$$\frac{\partial}{\partial t}S_{11}(k,t) = [-2M_{11}k^2(f_{11} + 2\kappa_{11}k^2) - 2M_{12}k^2(f_{21} + 2\kappa_{21}k^2)]S_{11}(k,t) + [-2M_{11}k^2(f_{12} + 2\kappa_{12}k^2) - 2M_{12}k^2(f_{22} + 2\kappa_{22}k^2)]S_{12}(k,t) \quad (42.a)$$

$$\frac{\partial}{\partial t}S_{12}(k,t) = [-M_{21}k^2(f_{11} + 2\kappa_{11}k^2) - M_{22}k^2(f_{21} + 2\kappa_{21}k^2)]S_{11}(k,t) + [-M_{11}k^2(f_{11} + 2\kappa_{11}k^2) - M_{12}k^2(f_{21} + 2\kappa_{21}k^2)]S_{12}(k,t) + [-M_{21}k^2(f_{12} + 2\kappa_{12}k^2) - M_{22}k^2(f_{22} + 2\kappa_{22}k^2)]S_{12}(k,t) + [-M_{11}k^2(f_{12} + 2\kappa_{12}k^2) - M_{12}k^2(f_{22} + 2\kappa_{22}k^2)]S_{22}(k,t) \quad (42.b)$$

$$\frac{\partial}{\partial t}S_{22}(k,t) = [-2M_{21}k^2(f_{11} + 2\kappa_{11}k^2) - 2M_{22}k^2(f_{21} + 2\kappa_{21}k^2)]S_{12}(k,t) + [-2M_{21}k^2(f_{12} + 2\kappa_{12}k^2) - 2M_{22}k^2(f_{22} + 2\kappa_{22}k^2)]S_{22}(k,t) \quad (42.c)$$

The above equations can be expressed in the matrix form as

$$\frac{\partial}{\partial t}[\mathbf{S}] = [\mathbf{A}]\cdot[\mathbf{S}] \quad (43)$$

where matrix [S] represents

$$\begin{bmatrix} S_{11}(k,t) \\ S_{12}(k,t) \\ S_{22}(k,t) \end{bmatrix}$$

and the components of matrix [A] are

$$A_{11} = -2M_{11}k^2(f_{11} + 2\kappa_{11}k^2) - 2M_{12}k^2(f_{21} + 2\kappa_{21}k^2)$$

$$A_{12} = -2M_{11}k^2(f_{12} + 2\kappa_{12}k^2) - 2M_{12}k^2(f_{22} + 2\kappa_{22}k^2)$$

$$A_{13} = 0$$

$$A_{21} = \frac{1}{2}A_{32}$$

$$A_{22} = \frac{1}{2}(A_{11} + A_{33})$$

$$A_{23} = \frac{1}{2}A_{12}$$

$$A_{31} = 0$$

$$A_{32} = -2M_{21}k^2(f_{11} + 2\kappa_{11}k^2) - 2M_{22}k^2(f_{21} + 2\kappa_{21}k^2)$$

$$A_{33} = -2M_{21}k^2(f_{12} + 2\kappa_{12}k^2) - 2M_{22}k^2(f_{22} + 2\kappa_{22}k^2) \quad (44)$$

The solution of the partial structure function is

$$[\mathbf{S}] = e^{[\mathbf{A}]\times t}\cdot[\mathbf{S}_o] \quad (45.a)$$

$e^{[A]t}$ can be calculated by

$$e^{[\mathbf{A}]\mathbf{x}t} = [\mathbf{P}]\cdot\begin{bmatrix} e^{\lambda_1 t} & 0 & 0 \\ 0 & e^{\lambda_2 t} & 0 \\ 0 & 0 & e^{\lambda_3 t} \end{bmatrix}\cdot[\mathbf{P}]^{-1} \quad (45.b)$$

where λ_i is the principal value and [P] is the matrix of the principal vectors. In (45.a), $[\mathbf{S}_o]$ is the matrix of the initial partial structure functions; i.e. the partial structure functions in the one-phase region.

$$[\mathbf{S}_o] = \begin{bmatrix} S_{11}(k,0) \\ S_{12}(k,0) \\ S_{22}(k,0) \end{bmatrix}$$

where

$$S_{11}(k,0) = \left[\frac{1}{\phi_1 P_{1w}} + \frac{1}{\phi_3 P_3} - 2\chi_o + \frac{k^2a^2}{18}\left(\frac{\overline{P_1^2}}{\phi_1 P_{1w}^2} + \frac{1}{\phi_3}\right)\right]^{-1} \quad (46.a)$$

$$S_{12}(k,0) = \left[\frac{1}{\phi_3 P_3} - 2\chi_o + \frac{k^2a^2}{18}\left(\frac{1}{\phi_3}\right)\right]^{-1} \quad (46.b)$$

$$S_{22}(k,0) = \left[\frac{1}{\phi_2 P_{2w}} + \frac{1}{\phi_3 P_3} - 2\chi_o + \frac{k^2a^2}{18}\left(\frac{\overline{P_2^2}}{\phi_2 P_{2w}^2} + \frac{1}{\phi_3}\right)\right]^{-1} \quad (46.c)$$

In the three-component model, the scattering intensity should be proportional to the linear combination of the three partial structure functions, i.e. $S(k,t) = S_{11}(k,t) + 2S_{12}(k,t) + S_{22}(k,t)$.

In Figures 1–3 we show $\Delta S/S(k,0)$ versus k^* for system 1 analyzed in the three-component model (see eq 27). When $\chi_f P$ is equal to 5.0, $\Delta S/S(k,0)$ is smaller than that in the two-component model at all k^*. Also the range of k^* where $\Delta S/S(k,0) > 0$ is smaller than 1.0, and k^*_{peak} is smaller than that in the two-component model. As $\chi_f P$ increases to 10, the range of k^* where $\Delta S/S(k,0) > 0$ is almost equal to 1.0, and $\Delta S/S(k,0)$ and k^*_{peak} become larger than those in the two-component model. We also can find k^*_{peak} decreases as $\chi_f P$ increases. As $\chi_f P$ is very large, the difference between the k^*_{peak} in the two- and the three-component models is found to be a constant 0.05.

In Figures 4–6 we show the results for system 2 (see eq 28). Basically, the results are similar to those for system 1: $\Delta S/S(k,0)$ becomes larger than that in the two-component model when $\chi_f P$ is greater than 9.0. As $\chi_f P$ is very large, the difference of k^*_{peak} between the two- and the three-component models is found to be a constant 0.04. In general, the difference between the two-component and three-component models decreases as the polydispersity index of polymer A decreases. When polymer A is monodisperse, the results in the two- and three-component models are exactly the same (see Figure 7).

II.3. Four-Component Model. In this model polymer A is divided into three polymer samples, 1–3 with equal average compositions and with weight-average degrees of polymerization P_{1w}, P_{2w}, and P_{3w}, respectively. Polymer sample 1 contains the chains whose degrees of polymerization are less than P^*. Polymer sample 2 contains the chains whose degrees of polymerization are between P^* and P^{**}. Those chains whose degrees of polymerization are greater than P^{**} belong to polymer sample 3. We determine P^* and P^{**} by the relation

$$\sum_{P=1}^{P^*} W_A(P) = \sum_{P=P^*}^{P^{**}} W_A(P) = \sum_{P=P^{**}}^{\infty} W_A(P) = \frac{1}{3} \quad (47)$$

where $W_A(P)$ is a normalized weight distribution. There-

fore P_{1w}, P_{2w}, and P_{3w} are given by

$$P_{1w} = \frac{\sum_{P=1}^{P^*} W_A(P) \times P}{\sum_{P=1}^{P^*} W_A(P)} \quad (48.a)$$

$$P_{2w} = \frac{\sum_{P=P^*}^{P^{**}} W_A(P) \times P}{\sum_{P=P^*}^{P^{**}} W_A(P)} \quad (48.b)$$

$$P_{3w} = \frac{\sum_{P=P^{**}}^{\infty} W_A(P) \times P}{\sum_{P=P^{**}}^{\infty} W_A(P)} \quad (48.c)$$

The free energy of mixing is

$$\Delta f = K_B T\left[\frac{\varphi_1^\circ \ln \varphi_1^\circ}{P_{1w}} + \frac{\varphi_2^\circ \ln \varphi_2^\circ}{P_{2w}} + \frac{\varphi_3^\circ \ln \varphi_3^\circ}{P_{3w}} + \frac{\varphi_4^\circ \ln \varphi_4^\circ}{P_4} + \chi(\varphi_1^\circ + \varphi_2^\circ + \varphi_3^\circ)\varphi_4^\circ\right] \quad (49)$$

and the spinodal curves are given by

$$\begin{vmatrix} f_{11} & f_{12} & f_{13} \\ f_{21} & f_{22} & f_{23} \\ f_{31} & f_{32} & f_{33} \end{vmatrix} = 0$$

with

$$f_{ii} = K_B T\left(\frac{1}{\varphi_i^\circ P_{iw}} + \frac{1}{\varphi_4^\circ P_4} - 2\chi\right) \quad i = 1\text{–}3 \quad (50.a)$$

$$f_{ij} = K_B T\left(\frac{1}{\varphi_4^\circ P_4} - 2\chi\right) \quad i \neq j, i, j = 1\text{–}3 \quad (50.b)$$

Expanding the determinant and using $\varphi_1^\circ = \varphi_2^\circ = \varphi_3^\circ = \varphi_A^\circ/3$ and $\varphi_1^\circ P_{1w} + \varphi_2^\circ P_{2w} + \varphi_3^\circ P_{3w} = \varphi_A^\circ P_{Aw}$, we find

$$2\chi_s = \frac{1}{\varphi_A^\circ P_{Aw}} + \frac{1}{\varphi_B^\circ P_B} \quad (51)$$

which is consistent with the two- and three-component models. Therefore, the critical conditions in the four-component model can be obtained simply from the two-component model.

System 1 analyzed in the four-component model is described by

$$P_{1w} = 354$$
$$P_{2w} = 849$$
$$P_{3w} = 1797$$
$$P_4 = 1000 \quad (52)$$
$$\varphi_{1c}^\circ = \varphi_{2c}^\circ = \varphi_{3c}^\circ = 0.1835$$
$$\varphi_{4c}^\circ = 0.4495$$
$$\chi_c P = 2.020\,62$$

and system 2 by

$$P_{1w} = 449$$
$$P_{2w} = 898$$
$$P_{3w} = 1653$$
$$P_4 = 1000 \quad (53)$$
$$\varphi_{1c}^\circ = \varphi_{2c}^\circ = \varphi_{3c}^\circ = 0.5359/3$$
$$\varphi_{4c}^\circ = 0.4641$$
$$\chi_c P = 2.010\,36$$

With this construction, the monodisperse polymer system becomes

$$P_{1w} = P_{2w} = P_{3w} = P_A = 1000$$
$$P_4 = 1000$$
$$\varphi_{1c}^\circ = \varphi_{2c}^\circ = \varphi_{3c}^\circ = 0.5/3 \quad (54)$$
$$\varphi_{4c}^\circ = 0.5$$
$$\chi_c P = 2$$

The partial structure functions in the four-component model may be derived by introducing three independent diffusion fluxes

$$J_i = -\sum_{k=1}^{3} M_{ik} \nabla(\mu_k - \mu_4) \qquad i = 1\text{–}3 \quad (55)$$

Substituting for $\mu_i - \mu_4$ in terms of f_{ij} and κ_{ij} (see eq 38), and using the conservation law, $\partial\varphi_i(r,t)/\partial t = -\nabla J_i$, we get

$$\frac{\partial}{\partial t}\varphi_i(r,t) = \sum_{k=1}^{3} M_{ik}\left[\sum_{j=1}^{3} f_{kj}\nabla^2\varphi_j(r,t) - 2\sum_{j=1}^{3}\kappa_{kj}\nabla^4\varphi_j(r,t)\right] = \sum_{k=1}^{3}\sum_{j=1}^{3} M_{ik}f_{kj}\nabla^2\varphi_j(r,t) - 2\sum_{k=1}^{3}\sum_{j=1}^{3} M_{ik}\kappa_{kj}\nabla^4\varphi_j(r,t) \quad (56)$$

$$i = 1\text{–}3$$

with

$$M_{11} = (1-\varphi_1^\circ)^2 M_1 + \varphi_1^{\circ 2} M_2 + \varphi_1^{\circ 2} M_3 + \varphi_1^{\circ 2} M_4$$

$$M_{12} = M_{21} = -(1-\varphi_1^\circ)\varphi_2^\circ M_1 - \varphi_1^\circ(1-\varphi_2^\circ)M_2 + \varphi_1^\circ\varphi_2^\circ M_3 + \varphi_1^\circ\varphi_2^\circ M_4$$

$$M_{13} = M_{31} = -(1-\varphi_1^\circ)\varphi_3^\circ M_1 + \varphi_1^\circ\varphi_3^\circ M_2 - \varphi_1^\circ(1-\varphi_3^\circ)M_3 + \varphi_1^\circ\varphi_3^\circ M_4$$

$$M_{22} = \varphi_2^{\circ 2} M_1 + (1-\varphi_2^\circ)^2 M_2 + \varphi_2^{\circ 2} M_3 + \varphi_2^{\circ 2} M_4$$

$$M_{23} = M_{32} = \varphi_2^\circ\varphi_3^\circ M_1 - \varphi_3^\circ(1-\varphi_2^\circ)M_2 - \varphi_2^\circ(1-\varphi_3^\circ)M_3 + \varphi_2^\circ\varphi_3^\circ M_4$$

$$M_{33} = \varphi_3^{\circ 2} M_1 + \varphi_3^{\circ 2} M_2 + (1-\varphi_3^\circ)^2 M_3 + \varphi_3^{\circ 2} M_4 \quad (57)$$

f_{ij} and κ_{ij} can be obtained by following the same steps as the two-component model (see Appendix), f_{ij} are given in

eq 50 and

$$\kappa_{ii} = K_B T\left[\frac{a^2}{36}\left(\frac{\overline{P_i^2}}{\mathring{\varphi}_i \mathring{P}_{iw}^2} + \frac{1}{\mathring{\varphi}_4}\right)\right] \quad i = 1\text{–}3 \quad (58.a)$$

$$\kappa_{ij} = K_B T\left[\frac{a^2}{36}\left(\frac{1}{\mathring{\varphi}_4}\right)\right] \quad i, j = 1\text{–}3;\ i \neq j \quad (58.b)$$

The equations of the time derivatives of the six partial structure functions are given in matrix form as

$$\frac{\partial}{\partial t}[\mathbf{S}] = [\mathbf{A}]\cdot[\mathbf{S}] \quad (59)$$

where

$$[\mathbf{S}] = \begin{bmatrix} S_{11}(k,t) \\ S_{12}(k,t) \\ S_{13}(k,t) \\ S_{22}(k,t) \\ S_{23}(k,t) \\ S_{33}(k,t) \end{bmatrix}$$

There are nine independent coefficients in [A]:

$$A_{11} = -2k^2\sum_{i=1}^{3} M_{1i}(f_{i1} + 2\kappa_{i1}k^2)$$

$$A_{12} = -2k^2\sum_{i=1}^{3} M_{1i}(f_{i2} + 2\kappa_{i2}k^2)$$

$$A_{13} = -2k^2\sum_{i=1}^{3} M_{1i}(f_{i3} + 2\kappa_{i3}k^2)$$

$$A_{42} = -2k^2\sum_{i=1}^{3} M_{2i}(f_{i1} + 2\kappa_{i1}k^2)$$

$$A_{44} = -2k^2\sum_{i=1}^{3} M_{2i}(f_{i2} + 2\kappa_{i2}k^2)$$

$$A_{45} = -2k^2\sum_{i=1}^{3} M_{2i}(f_{i3} + 2\kappa_{i3}k^2)$$

$$A_{63} = -2k^2\sum_{i=1}^{3} M_{3i}(f_{i1} + 2\kappa_{i1}k^2)$$

$$A_{65} = -2k^2\sum_{i=1}^{3} M_{3i}(f_{i2} + 2\kappa_{i2}k^2)$$

$$A_{66} = -2k^2\sum_{i=1}^{3} M_{3i}(f_{i3} + 2\kappa_{i3}k^2) \quad (60.a)$$

The other dependent coefficients are given by

$$A_{22} = \frac{A_{11} + A_{44}}{2}$$

$$A_{33} = \frac{A_{11} + A_{66}}{2}$$

$$A_{55} = \frac{A_{44} + A_{66}}{2}$$

$$A_{21} = A_{53} = \frac{A_{42}}{2}$$

$$A_{23} = A_{56} = \frac{A_{45}}{2}$$

$$A_{24} = A_{35} = \frac{A_{12}}{2}$$

$$A_{25} = A_{36} = \frac{A_{13}}{2}$$

$$A_{31} = A_{52} = \frac{A_{63}}{2}$$

$$A_{32} = A_{54} = \frac{A_{65}}{2}$$

$$A_{14} = A_{15} = A_{16} = 0$$

$$A_{26} = 0$$

$$A_{34} = 0$$

$$A_{41} = A_{43} = A_{46} = 0$$

$$A_{51} = 0$$

$$A_{61} = A_{62} = A_{64} = 0 \quad (60.b)$$

In the four-component model, the scattering intensity is proportional to the linear combination of the partial structure functions, i.e. $S(k,t) = S_{11}(k,t) + 2S_{12}(k,t) + 2S_{13}(k,t) + S_{22}(k,t) + 2S_{23}(k,t) + S_{33}(k,t)$ where the partial structure functions at a given time in the early stages can be calculated from

$$[\mathbf{S}] = e^{[\mathbf{A}]\times t}\cdot[\mathbf{S}_0] \quad (61)$$

where the initial partial structure functions are given by

$$S_{ii}(k,0) = \left[\frac{1}{\mathring{\varphi}_i \mathring{P}_{iw}} + \frac{1}{\mathring{\varphi}_3 \mathring{P}_3} - 2\chi_o + \frac{k^2a^2}{18}\left(\frac{\overline{P_i^2}}{\mathring{\varphi}_i \mathring{P}_{iw}^2} + \frac{1}{\mathring{\varphi}_3}\right)\right]^{-1}$$

$$i = 1\text{–}3 \quad (62.a)$$

$$S_{ij}(k,0) = \left[\frac{1}{\mathring{\varphi}_3 \mathring{P}_3} - 2\chi_o + \frac{k^2a^2}{18}\left(\frac{1}{\mathring{\varphi}_3}\right)\right]^{-1}$$

$$i \neq j;\ i, j = 1\text{–}3 \quad (62.b)$$

In Figures 1–3 we show $\Delta S/S(k,0)$ versus k^* for system 1 analyzed in the four-component model (see eq 52). When $\chi_f P$ is equal to 5.0, $\Delta S/S(k,0)$ is the smallest, and the range of k^* where $\Delta S/S(k,0) > 0$ is the narrowest of the three different component models. As $\chi_f P$ increases to 10, $\Delta S/S(k,0)$ is larger than that in the two-component model in the region of k^* between 0 and 0.8 but still smaller than that in the three-component model. We can find, when $\chi_f P$ reaches 20, $\Delta S/S(k,0)$ begins to be the largest compared with the results of two- and three-component models. In general, k^*_{peak} decreases as $\chi_f P$ increases. The region over which k^*_{peak} is found is between 0.53 and 0.27 when $\chi_f P$ is in between 5.0 and 100. Comparing the values of k^*_{peak} obtained in the three- and four-component models, the difference of k^*_{peak} stays about 0.02 when $\chi_f P$ is very large.

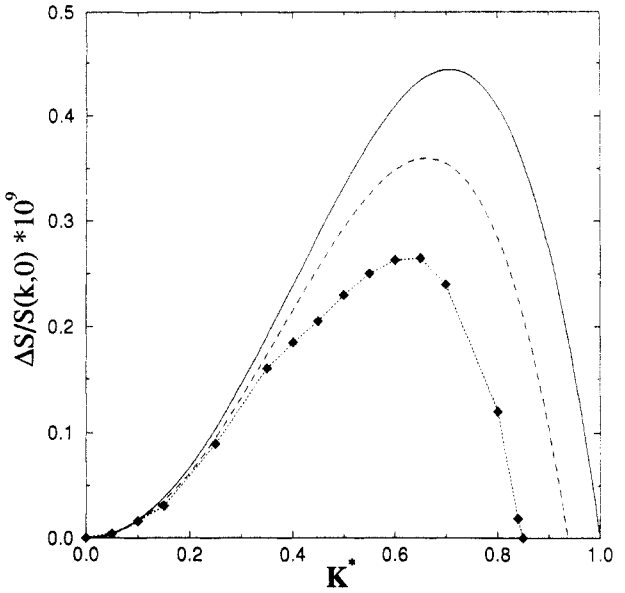

Figure 8. Normalized structure function of the polydisperse polymer blend 1 described in eq 8 with k-independent Onsager coefficients (see eq 13.a) for quenches from $\chi_o = 0$ to $\chi_f P = 5.0$ for $t = 1$. The symbols —, - - -, and ♦···♦ correspond to the two-, three-, and four-component models, respectively, and $k^*_{peak} = 0.71$, 0.66, and 0.65, respectively.

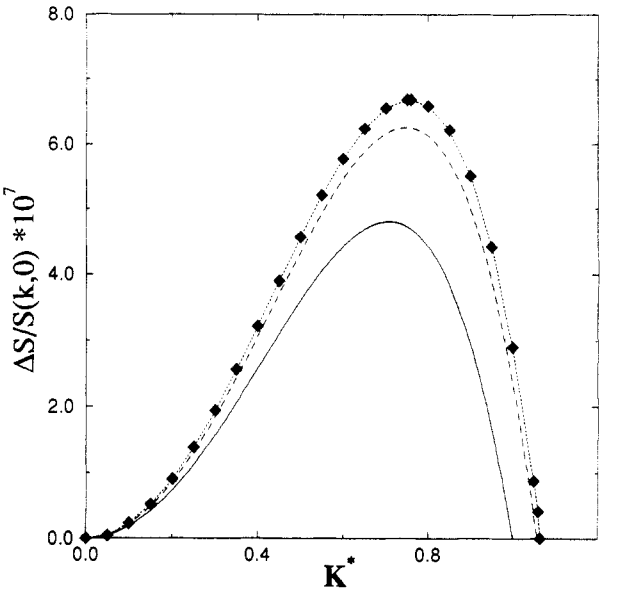

Figure 9. Normalized structure function of the polydisperse polymer blend 1 described in eq 8 with k-independent Onsager coefficients (see eq 13.a) for quenches from $\chi_o = 0$ to $\chi_f P = 100$ for $t = 1$. The symbols —, - - -, and ♦···♦ correspond to the two-, three-, and four-component models, respectively, and $k^*_{peak} = 0.71$, 0.75, and 0.76, respectively.

In Figures 4–6 we show the results for system 2 analyzed in the four-component model (see eq 53): Compared with Figures 1–3, the difference between the results analyzed in the three- and four-component models is smaller. The difference between the k^*_{peak} in the three- and four-component models is about 0.01 with very large $\chi_f P$. In Figure 7, we also show the result for the monodisperse system analyzed in the four-component model (see eq 54), which is exactly the same as in the two- and three-component models.

III. Discussion

In order to determine the effect of k dependence in the form used for M_i in eq 13.a, we run the numerical solutions for all of the cases discussed in the previous section using M_i in eq 13.b, i.e. a wavevector-independent Onsager coefficient. In Figures 8 and 9 we plot $\Delta S/S(k,0)$ versus k^* for the polydisperse A–monodisperse B system (1) (see eq 8) in the two-, three-, and four-component models for $\chi_f P = 5.0$ and $\chi_f P = 100$. In this case we found no shift in k^*_{peak} for the two-component model, while k^*_{peak} increases as χ_f increases for the three- and four-component models.

IV. Conclusions

Polydispersity effects in the thermodynamics and the early stages of the phase separation dynamics in incompatible monodisperse A–monodisperse B and polydisperse A–monodisperse B polymer blends have been studied. The polymer blend is analyzed as a two-, three-, and four-component model by dividing polymer A into one, two, and three samples, respectively. The samples are characterized by the average degree of polymerization. We analyze numerically two polydisperse systems. Both systems 1 and 2 have the Schulz–Flory distribution with polydispersity indices $\gamma_A = 2.0$ and $\gamma_A = 1.5$, respectively. We find that when polymer A is monodisperse, the results of thermodynamics and dynamics analyzed in the three different models are the same, in this case there is only one independent structure function which can represent the scattering intensity in a scattering experiment. When polymer A is polydisperse, however, the dynamics are not described by the standard way of analyzing polydispersity effects: using a two-component model where the effects of a distribution of degrees of polymerization are only included through the weight-average degree of polymerization of the polymer A.

Our results are explained by kinetic effects. When the driving force which causes the phase separation is small, that is when the quench size $\Delta\chi = |\chi_c - \chi_f|$ is small, the long chains cannot diffuse completely and seem "frozen" in the early stages, which will cause a smaller scattering intensity and k^*_{peak} in the four and three-component models with respect to the two-component model. As $\Delta\chi$ increases to larger values, the long chains are no longer frozen in the early stages and cause a larger scattering intensity and k^*_{peak} of the four- and three-component models with respect to the two-component model. This observation is independent of which model we use for the Onsager coefficients of the various components (see eq 13.a or eq 13.b), as expected.

Acknowledgment. This research was supported by the National Science Foundation (PYI Grant No. DMR 9057764), the David and Lucile Packard Foundation, and the Ford Motor Co. We thank Prof. G. B. Olson for suggesting to us application of the multicomponent model to study polydisperse polymer blends.

Appendix

The gradient-energy coefficient κ in the polydisperse polymer A–monodisperse polymer B blends can be obtained by calculating the structure function $S_{AA}(k)$ in the one-phase region using the random phase approximation

method:[20,21]

$$S_{AA}(k) = \left[\frac{1}{\mathring{\varphi}_A G_A(P_{Aw},k)} + \frac{1}{\mathring{\varphi}_B G_B(P_B,k)} - 2\chi\right]^{-1} \quad \text{(A.1a)}$$

where

$$G_B(P_B,k) \equiv \frac{1}{P_B}\sum_{n,m=1}^{P_B}\langle \exp[ik\cdot(R_n - R_m)]\rangle = P_B \times f(k^2 R_g^2) \quad \text{(A.1b)}$$

$$G_A(P_{Aw},k) = \frac{1}{\mathring{\varphi}_A}\sum_{\alpha=1}^{\alpha=n_A}\varphi_A^\alpha G_A^\alpha(P_\alpha,k) \quad \text{(A.1c)}$$

n_A is the total number of chains of polymer A, $f(x)$ is the Debye function,

$$f(x) = \frac{2}{x^2}(e^{-x} - 1 + x) \quad \text{(A.2)}$$

and R_g^2 is the mean square radius of gyration. Expanding $G(P,k)$ for $|kR_g| \ll 1$ and assuming the mean lengths of segments A and B are the same as a yield

$$G_A(P_{Aw},k) = P_{Aw}\left(1 - \frac{k^2a^2}{18}\frac{\overline{P_A^2}}{P_{Aw}}\right) \quad \text{(A.3a)}$$

$$G_B(P_B,k) = P_B\left(1 - \frac{k^2a^2}{18}P_B\right) \quad \text{(A.3b)}$$

where

$$\overline{P_A^2} = \frac{\sum_{\alpha=1}^{n_A}(P_A^\alpha)^3}{\sum_{\alpha=1}^{n_i}(P_A^\alpha)} \quad \text{(A.3c)}$$

Substituting eq A.3 into eq A.1a can yield an expression of $S_{AA}(k)$ in the form

$$S_{AA}(k) = \left[\frac{1}{\mathring{\varphi}_A P_{Aw}} + \frac{1}{\mathring{\varphi}_B P_B} - 2\chi + \frac{k^2a^2}{18}\left(\frac{\overline{P_A^2}}{\mathring{\varphi}_A P_{Aw}^2} + \frac{1}{\mathring{\varphi}_B}\right)\right]^{-1} \quad \text{(A.4)}$$

In the Cahn–Hilliard–Cook equation, the structure function in the one-phase region as $t \to \infty$ is given by

$$S_{AA}(k) = K_B T[f'' + 2\kappa k^2]^{-1} \quad \text{(A.5)}$$

Combining eqs A.4 and A.5,

$$f'' = K_B T\left(\frac{1}{\mathring{\varphi}_A P_{Aw}} + \frac{1}{\mathring{\varphi}_B P_B} - 2\chi\right) \quad \text{(A.6a)}$$

$$\kappa = K_B T\left[\frac{a^2}{36}\left(\frac{\overline{P_A^2}}{\mathring{\varphi}_A P_{Aw}^2} + \frac{1}{\mathring{\varphi}_B}\right)\right] \quad \text{(A.6b)}$$

References and Notes

(1) Edwards, S. F. *J. Phys.* **1975**, *A8*, 1670.
(2) de Gennes, P. G. *J. Phys. (Paris) Lett.* **1977**, *L38*, 441.
(3) Cahn, J. W.; Hilliard, J. E. *J. Chem. Phys.* **1958**, *28*, 258.
(4) Cahn, J. W.; Hilliard, J. E. *J. Chem. Phys.* **1959**, *31*, 688.
(5) de Fontaine, D. Doctoral dissertation, Northwestern University, Evanston, IL, 1967.
(6) Koningsveld, R.; Kleintjens, L. A. *J. Polym. Sci. Polym. Symp.* **1977**, *61*, 221.
(7) Langer, J. S.; Baron, M.; Miller, H. D. *Phys. Rev.* **1975**, *A11*, 1417.
(8) Cook, H. E. *Acta Metall.* **1970**, *18*, 297.
(9) Rundman, K. B.; Hilliard, J. E. *Acta Metall.* **1967**, *15*, 1025.
(10) Takenaka, M.; Hashimoto, T. *Phys. Rev.* **1993**, *E48*, R647.
(11) Schaefgen, J. R.; Flory, P. J. *J. Am. Chem. Soc.* **1948**, *70*, 2709.
(12) Schulz, G. V. *Z. Phys. Chem.* **1939**, *B43*, 25.
(13) de Gennes, P. G. *J. Chem. Phys.* **1980**, *72*, 4756.
(14) Kramer, E. J.; Green, P.; Palstrom, C. J. *Polymer* **1984**, *25*, 473.
(15) Composto, R. J.; Kramer, E. J.; White, D. M. *Nature* **1987**, *328*, 234.
(16) In polymer blends of comparable molecular weights, the results of Kramer and de Gennes are similar (see discussions in the paper of Jangweon Rhee and Buckley Crist (*Macromolecules* **1991**, *24*, 5663)).
(17) Pincus, P. *J. Chem. Phys.* **1981**, *75*, 1996.
(18) Binder, K. *J. Chem. Phys.* **1983**, *79*, 6387.
(19) Hoyt, J. J. *Acta Metall.* **1989**, *37*, 2489.
(20) Joanny, J. F. *C. R. Acad. Sci. Paris* **1978**, *286B*, 89.
(21) de Gennes, P. G. Scaling Concepts in Polymer Physics; Cornell University Press: Ithaca, NY, 1979.